APPLIED
MATERIALS
AND TECHNOLOGY

Research Article

Jamt.ejournal.unri.ac.id

Exploring the Potentials and Drawbacks of Hysteresis Current Controller for SRM: A Case Study of Wind Energy Conversion System

Imamuddeen Kabir*, Yusuf Jibril , Adamu Sa'idu Abubakar , Gbenga Abidemi Olarinoye

Department of Electrical Engineering, Ahmadu Bello University, Zaria Nigeria

ABSTRACT: DSwitched Reluctance Machines (SRMs) have drawn interest in renewable energy systems because of their special qualities and applicability. This study examines the idea of hysteresis current regulation in a wind energy conversion system with a Switched Reluctance Generator (SRG). The system is modeled in MATLAB/SIMULINK. The model is simulated and analyzed to ascertain the system's benefits and shortcomings, focusing on reducing torque ripples in SRG. Considering most classical controllers are complicated to construct, the hysteresis current control is straightforward and effective. However, this controller's two primary shortcomings are that it produces a variable switching frequency and increases current ripples at a steady state, both enhancing acoustic noise in SRM. Lastly, the report suggests that improving controller performance should be the primary emphasis of future research in this field.

Key words: Switched reluctance generator, wind turbine, MPPT, phase commutation controller, hysteresis current controller (HCC).

1. INTRODUCTION

In recent years, several Switched Reluctance Motors (SRMs) have proven effective in a variety of renewable energy applications such as Wind energy conversion Systems (WECS) [1], solar water pumping systems [2], electric vehicles [3], and small-scale hydropower plants [4]. SRMs possess distinct features like ease of manufacturing, resilience, and variable-condition efficiency that render them appropriate for various uses in renewable energy systems, particularly in direct drive applications [5]. Because the rotor lacks magnets and has windings, this machine possesses the lowest production cost. However, torque pulsation and acoustic noise are the SRM's principal shortcomings, which constrain their application. The right machine design and controller can significantly mitigate these drawbacks [6].

One of the most researched topics in power converter management is current control. In recent years, a lot of attention has been paid to two classic control strategies: Using pulse width modulation (PWM), hysteresis control, and linear control [7]. SRMs use a technique called hysteresis current control to control motor currents. It entails comparing the predefined upper and lower limits with the actual current. The frequency-altering problem of the hysteresis-type current controller limits its use in many applications where switching-related auditory disturbance is undesirable, even though it generally performs better dynamically. The observation by [8] supports this argument because the conventional control technique is affected by changes in plant parameters and operating conditions. Power converters and SRM drives can be controlled using several existing control systems that have been presented. The three-phase 6/4 switching reluctance generator (SRG) hysteresis current control (HCC) method presented in [9] is founded on electromagnetic field finite element analysis (FEA) and the nonlinear inductance model. In [10], a novel current control strategy for regulating the generator phase currents with the help of a hysteresis current controller is presented, demonstrating the operation of a switched reluctance generator-based wind energy conversion system (WECS) that can generate the maximum power under variable wind speed conditions. A thorough strategy utilizing switched reluctance generators (SRG) for variable wind energy conversion systems was presented in [11]. The authors suggest two different approaches to direct power control (DPC): one that operates at low speeds by using the SRG phase current's hysteresis, and another that operates at high speeds by using a single current pulse. A wind energy conversion system based on switching reluctance generators and featuring maximum power tracking was suggested in [12]. The wind turbine can follow its maximum power point by measuring wind speed to determine the optimal tip speed ratio.

Received : May 2, 2024
Revised : September 3, 2024
Accepted : September 8, 2024

Integrating renewable energy systems and SRG drives requires multiple components and sub-systems. MATLAB®/ Simulink software is used in this paper to model and simulate an SRM-based WECS. It offers toolboxes specifically for electrical drives, power electronics, and control systems, which can help analyze the performance of hysteresis current controllers under various operating conditions and with different renewable energy sources.

2. METHODOLOGY

To ascertain the general practicality of the strategy, the following stages are taken in order to attain a scientific approach to this notion.

- Modeling the SRM
- Modeling the Wind Energy Conversion System
- Modeling the Hysteresis current controller
- SRM based Wind turbine system simulation

2.1 Modeling the SRM

Figure 1 depicts a cross-sectional view of an 8/6 SR machine with four phases. It features six rotor poles and eight stator poles (A, A', B, B', C, C', D, D'). Assuming that the phase coupling between phases is accurate, the voltage across the SRM's phase terminals is as follows [13]:

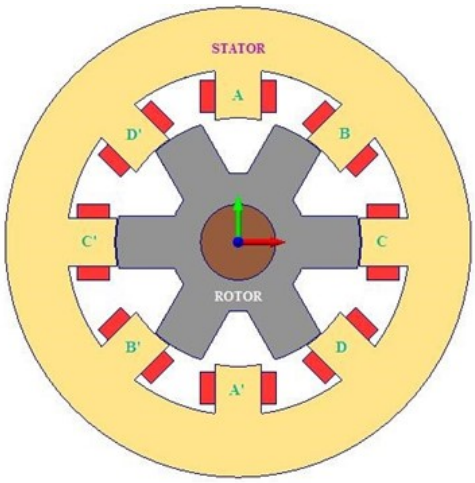

Fig. 1. An 8/6 switched reluctance machine's cross section

$$v_i = Ri + \frac{d\psi}{dt} = Ri + \omega_m \frac{d\psi}{d\theta} \quad (1)$$

$$v_i = Ri + \omega_m \frac{d(Li)}{d\theta} = Ri + L\frac{di}{dt} + \omega_m i\frac{dL}{d\theta} \quad (2)$$

Where θ depicts the location of the rotor., ω_m the angular velocity is expressed in rad/sec., R is the phase resistance, L is the phase inductance, and i is the current. The back-EMF (e) is the final term in equation (3).

$$e = \omega_m i\frac{dL}{d\theta} \quad (3)$$

The magnetic stored energy's rate of change at any given time is provided by:

$$\frac{d}{dt}\left(\frac{1}{2}Li^2\right) = \frac{1}{2}i^2\frac{dL}{dt} + Li\frac{di}{dt} = \frac{1}{2}i^2\omega_m Li\frac{di}{dt} \quad (4)$$

According to the principle of energy conservation, the mechanical power used in each phase is supplied by [14]:

$$P = \omega_m T_e \quad (5)$$

where, in each phase's toque is represented by T_e. This remains after the instantaneous electromagnetic torque, T_e is deducted from the power input V_i, along with the resistive loss (Ri). As a result, using equation (3) and (4), we write [15]:

$$T_e = p/\omega_m = vi - Ri^2 - d(1/2Li^2)/dt \quad (6)$$

$$T_e = \frac{1}{2}i^2\frac{dL}{d\theta} \quad (7)$$

The idea that a magnetic substance would often align itself to the minimal reluctance location in a magnetic field underlies the torque production in an SR machine. The stator pole is excited when the magnetic flux lines are at their smallest length and the rotor and stator poles are aligned in the generating mode [16].

2.2 Modeling the Wind Energy Conversion System

Nonlinear torque and power coefficients that are influenced by wind speed, pitch angle of the wind turbine blades, and rotor rotation speed, serve as indicators of aerodynamic nonlinearity. Therefore, maximum power point tracking (MPPT) is required for a wind turbine in order to continually lock to the ideal generator speed that guarantees the extraction of maximum power [17].

Turbine blades are designed aerodynamically to capture the most energy from the wind at wind speeds ranging from 3 to 15 m/s. In severe winds of approximately 15 to 25 m/s, the turbine needs to be aerodynamically strengthened in order to avoid damage [18]. In joules, the mass m's kinetic energy traveling at speed v_a in air provided by [19]:

$$KE = \frac{1}{2}mV^2 \quad (8)$$

The flow rate of kinetic energy per second in watts is used to calculate the power in flowing air:

$$P = \frac{1}{2}(mass\ flow\ per\ second)V^2 \quad (9)$$

The rate of volumetric flow is AV, in kilograms per second, the air's mass flow rate is ρAV, when the turbine's input mechanical power is [20]:

$$P_i = \frac{1}{2}(\rho AV)V^2 = \frac{1}{2}\rho AV^3 \quad (10)$$

The output wind mechanical power is given by:

$$P_m = \frac{1}{2}\rho AV^3 C_p(\lambda, \beta) \quad (11)$$

The effectiveness of a wind generator is dependent on two factors: the tip speed ratio, λ, and the coefficient of power C_p.

$$\lambda = \frac{\omega R}{V} \quad (12)$$

where:

ω = is the speed of the wind turbine shaft
β = is the pitch angle of the rotor
P = air movement-based mechanical force (watts)
ρ = air density (kg/m^3)
A = area that the rotor blades sweep (m^2), and
V = air movement speed (m/sec)

Fig. 2.4 displays the C_p-λ characteristics for various values of the pitch angle β. For $\beta = 0°$ and $\lambda = 8.1$, the maximum value of C_p ($C_p$max = 0.48) is reached. The nominal value λ_{nom} is the definition of this value of λ. For an optimal value of λ_{nom}, C_p and P_m are maximal.

The goal is to maximize power generation within the specified speed range while using SRG for wind energy applications [21]. Thus, the MPPT algorithm is integrated into the development of the wind turbine model [22]. Figure 5 displays the power that the wind turbine contributes at various wind velocities along an ideal line.

2.3 Hysteresis Current Controller

Hysteresis current and phase commutation controllers are included in the current controller. The phase commutation controller interpolates over the whole speed range after modifying θ_{on} and θ_{off} for the lowest torque ripples at particular speeds, enabling the phase at the proper angular location. The values of θ_{on} and θ_{off} correspond to both motoring and generating modes [23]. The machine phase switches are enabled and disabled based on the real current values by the hysteresis current controller.

The Switched Reluctance Machine (SRM) block receives a logic signal from the SRM Commutation Logic block. When to turn on and off the supply for each phase is indicated by the signal. For every phase, the commutation signal is:

1 if $\theta_{on} \le \theta_{ph} \le \theta_{off}$
0 if $\theta_{ph} < \theta_{on}$
0 if $\theta_{on} > \theta_{off}$

Where :

θ_{ph} is interval's phase angle $[0, \beta]$.
β is the angle of torque capability.
θ_{on} is the angle of switch-on.
θ_{off} the angle of switch-off.

The hysteresis boundary is defined as [6]:

$$B_{up} = I_{ref}(t) + \frac{B_w}{2}$$
$$B_{low} = I_{ref}(t) - \frac{B_w}{2} \quad (13)$$

where $I_{ref}$is the reference current, B_{up} is the upper boundary It is possible to evaluate the ripple current Δi as:

$$\Delta i \approx \frac{NT_s|U_{dc} - Ri - E|}{L_{inc}} \quad (14)$$

where, the phase's incremental inductance is called L_{ino}, the back-emf is called E, the phase's resistance is called R_i, the quantity of successive sample instances that the phase is provided with a steady voltage called NT_s, and the electric drive's voltage supply is called Udc. Because of the long sample time, the current in real time may surpass the designated bandwidth ΔH. Figure 3 illustrates how a chopper in the hysteresis band $I + (Ai/2)$ maintains the current at roughly constant levels. The incremental inductance L_{inc} controls the rate at which the current swings around the necessary level. The immediate rotor position can be inferred indirectly from the chopping characteristics since the incremental inductance depends on the rotor position.

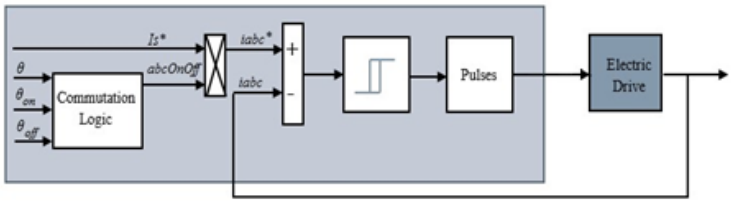

Fig. 2. Hysteresis current controller

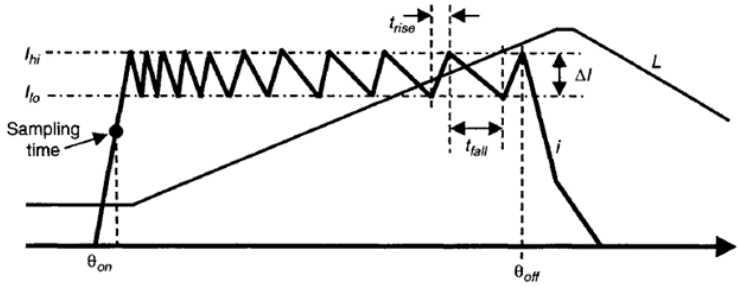

Fig. 3. Chopped current in active phase

The fundamental need is to regulate the SRM so that, at all angles, the machine torque, whether actual or measured, is precisely equal to the desired or reference torque. To effectively eliminate torque ripple, the machine's desired torque is adjusted as a function of electrical angle. Mathematically,

$$T_{ref} = T_{actual} + T_{ff} \quad (15)$$

where, T_{ref} is the reference torque, T_{actual} is the measured torque and T_{ff} is the feed forward torque. Ideally, the feed-forward torque $T_{ff}(0)$ is 180 ° out of phase with the torque tipple [24]. However, owing to nonlinear effects of the hysteresis controller, this will not be strictly true.

Hysteresis current control has several benefits and drawnbacks when used in Switched Reluctance Machines [25]:

Advantages:

No Current Regulation Loop: Hysteresis control eliminates the need for an additional control loop by immediately switching the converter devices (such as MOSFETs) based on the current error, in contrast to typical control methods that call for a current regulation loop.

Fast Response: Because it is designed to switch based on instantaneous error, it responds quickly to changes in load or operational conditions.

No Steady-State Error: Since hysteresis controllers function inside a defined range surrounding the reference value, they naturally remove steady-state errors. This feature can make system tweaking and stability issues easier to understand.

Drawbacks:

Variable Switching Frequency: Depending on the operational environment, the switching frequency can change, which makes filter design and electromagnetic interference (EMI) management difficult.

Increased Switching Losses: Overall efficiency may be impacted by the fluctuating and occasionally high switching frequency due to increasing switching losses.

Nonlinear Behavior: Hysteresis controllers' switching characteristics have the potential to induce nonlinearities into the control system. Because of its nonlinearity, stability and performance margins must be carefully considered in analysis and design.

In conclusion, hysteresis current controllers have drawbacks with regard to bandwidth, switching frequency effects, and nonlinear behavior even if they provide simplicity, quick response, and robustness. Their appropriateness is contingent upon the particular demands of the SRG application and the balance between complexity and performance.

2.4 Simulation Model of the SRM-Based WECS

Through the gear arrangement, the torque produced by the wind generator is combined with the SRM system to create an SRG-based method for converting wind energy. The suggested SRM-based wind power system is modeled and developed using Matlab®/Simulink modeling tools. The system's fundamental parts are the turbine model, the MPPT controller, the speed controller, the SRM, the hysteresis current controller and its related components, and the speed controller. The two most difficult operating conditions were used to simulate the hysteresis current controller's steady state performance. Figure 4 shows the wind power conversion system's SRM-using MATLAB/ Simulink model.

3. RESULT AND DISCUSSIONS

The rated velocity of 12 m/s and the cut-in velocity of 4 m/s are considered when modeling the WT. The suggested SRG WECS results at 12.5 m/s wind velocity are shown in Figures 5 and 6. Figure 5 shows that wind speed is increased rapidly from the initial speed of 10m/s to 12m/s at 0.5 s then gradually decreased to 8m/s at 1s intervals.

The inverter's voltage command is updated at the conclusion of every time interval in the control loop in the digital implementation of the hysteresis current controller. The performance of the controller could be examined thanks to the parallel collection of the reference current and the observed phase current. Throughout the entire digital time period, the current may diverge from its reference, which will amplify the torque ripple, particularly while transitioning from one phase to the next. Figures 7 and 8 display the stator current and electrical torque, respectively. A simulation validation of the hysteresis current controller's tracking

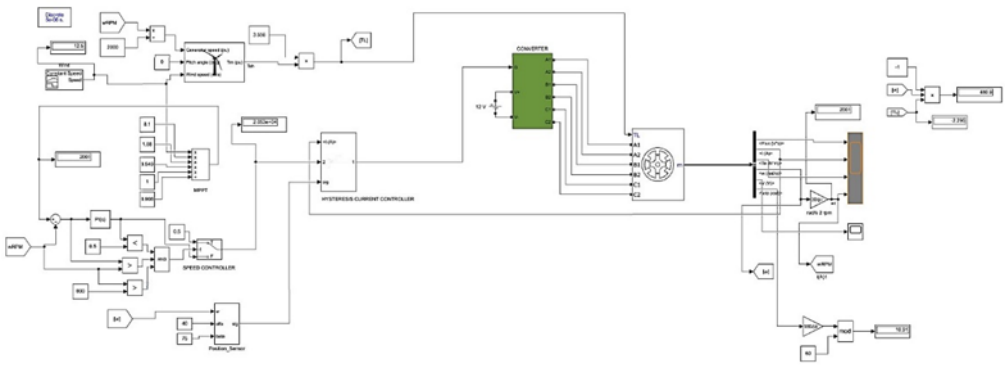

Fig. 4. Simulink model of wind energy conversion systems based on SRM

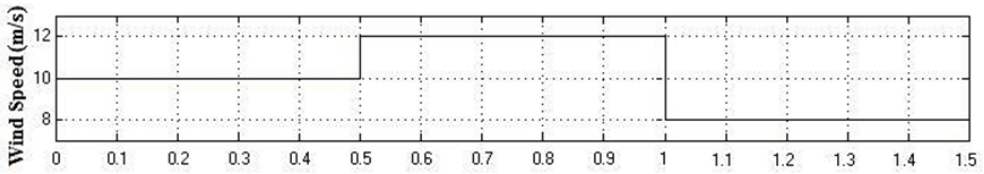

Fig. 5. Wind speed against time

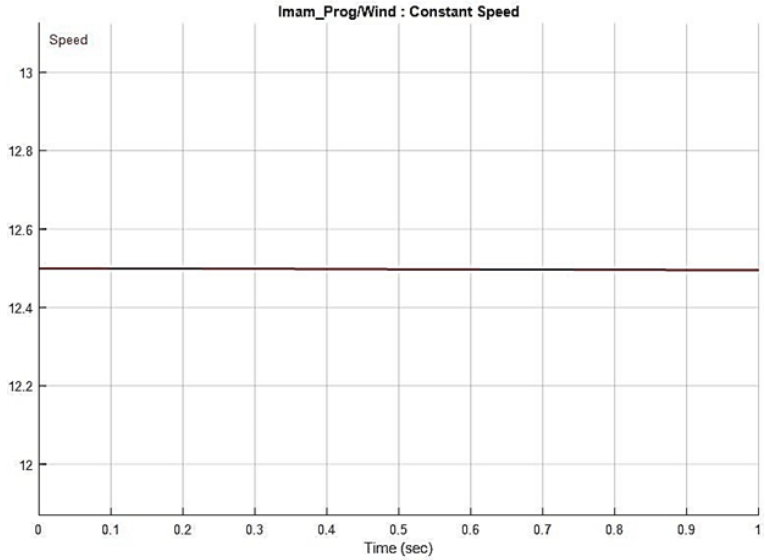

Fig. 6. Wind speed graph

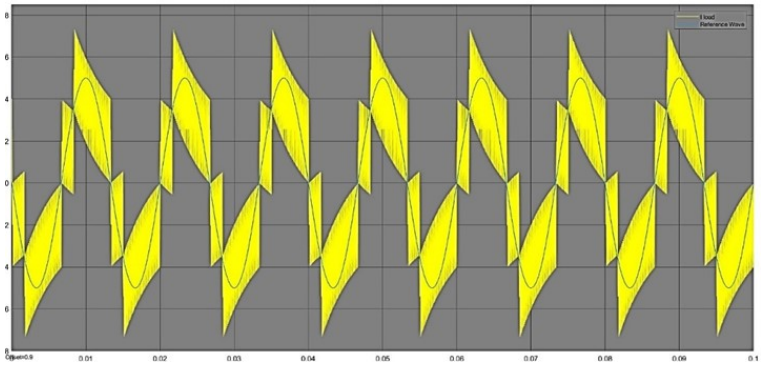

Fig. 7. The plot of reference and measured current

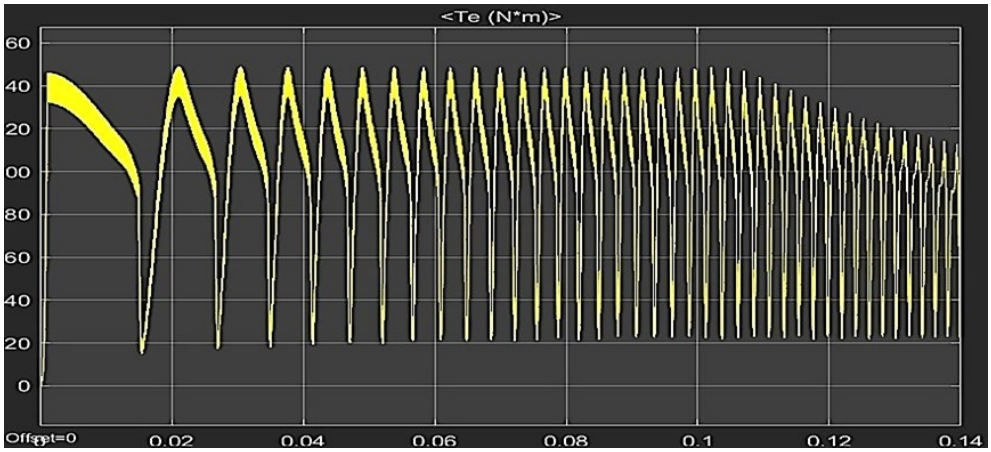

Fig. 8. Waveform of electrical torque

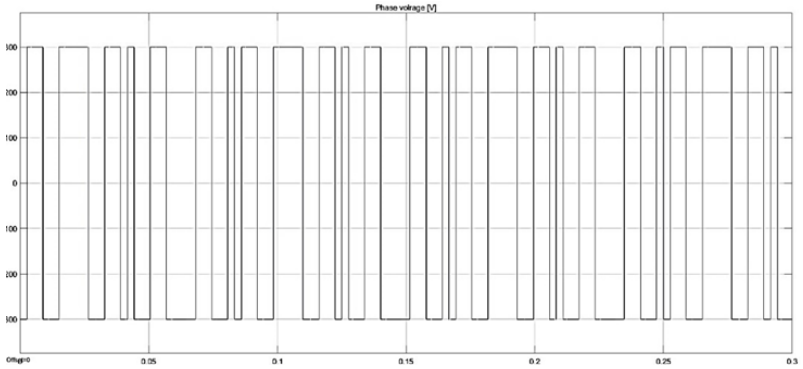

Fig. 9. Waveform of the output voltage

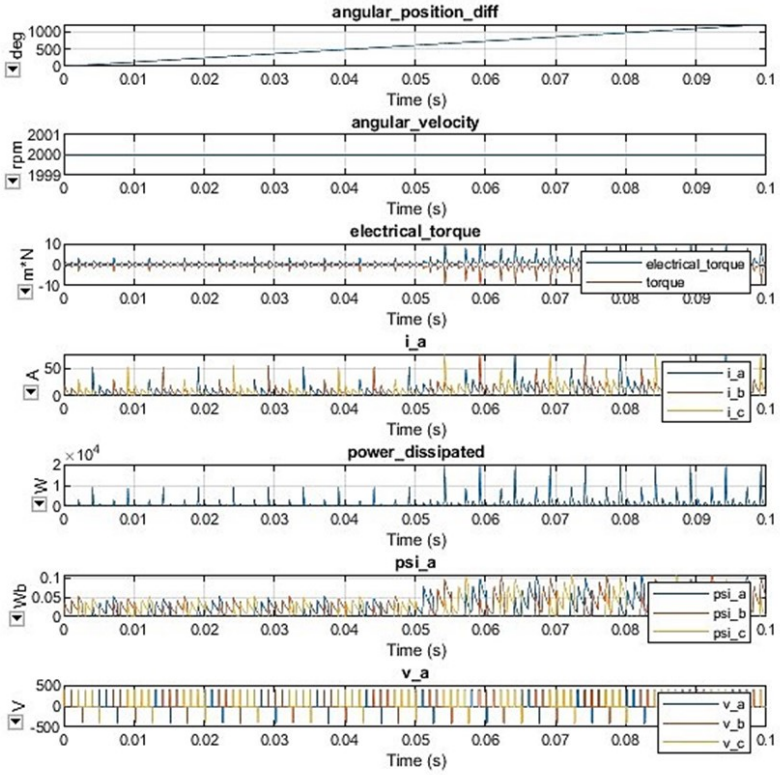

Fig. 10. (a to f): Waveforms of the SRM

performance using a sine wave reference signal was conducted. Except a little deviation, the current controllers on both axes can quickly respond to dynamics and follow their respective references. The actual current in one phase of the SRM is shown in yellow in the figures, while the reference current, which is equal to 5 A in the blue figures, produces an average electromagnetic torque T_e of 40 Nm at 2000 rpm.

In an electrical cycle, current commutation is primarily responsible for the torque dips, while saturation and the nonlinear nature of torque resulting from single-phase stimulation are the causes of the rounded peaks. Torque is generated in SRMs by drawing the rotor to the point that is aligned with the least amount of resistance through the application of current to a phase winding. The torque decreases from 40 Nm to 20 Nm between 0.1 and 0.14 seconds.

Acoustic noise issues could arise if the inverter's switching frequency falls within the audible range. The output voltage waveform in figure 9, which yields a square waveform, displays the fluctuations in switching frequency. It demonstrates that the switching frequency is maintained at roughly 15 kHz and that the square waveform's ON and OFF times are related to the inaccuracy in maintaining the switching frequency constant. There is variation in the switching frequency. This figure shows that the waveform, with time ON=0.038 seconds and time OFF=0.028 seconds, has an uneven mark-space ratio.

Figure 10 displays the reaction of the SRM for angular velocity, electric torque, power dissipated, phase currents, and phase voltages in the steady state. Figure 10 (a) shows the rotor's angular position with regard to Phase A, which ranges from zero to sixty degrees. The angular velocity, or rotor speed, of SRG is shown in Figure 10 (b). The instantaneous electrical torque, T_e, produced by the SRG is shown in Figure 10 (c). To represent phase voltages, the colors blue, red, and green are utilized., flux connections, phase currents, and power dissipated for phases A, B, and C in Figure 10(d), (e), (f), and (g), respectively. The phase windings' flux connections are depicted in figure 10 (f), where they increase from zero θ_{on} to a rated value of 0.3 in relation to the aligned position, then upon the phase current's return to zero, decrease once more to zero. Figure 10 (c) displays the entire electric torque, T_e produced by the SRG. Figure 10 (e) displays the average power that the load has available, while the 3-phase output voltage is shown in figure 10 (f).

4. CONCLUSION

Hysteresis current control has several possible applications, as previously indicated. All combined technologies have demonstrated their dependability as well as, naturally, their shortcomings. Hysteresis current control in SRM is highly favored for its responsiveness to load variations, built-in overcurrent protection, and less susceptibility to parameter changes. However, at steady state, this kind of control creates current ripples and generates a variable switching frequency, both of which amplify acoustic noise in SRM. This paper suggests that future research in this area should concentrate on improving the controller performance of the SRM to more closely monitor the reference phase current throughout the machine's whole operating speed range at a constant PWM switching frequency. This will provide a convincing argument for its inclusion in renewable energy systems.

AUTHOR INFROMATION

Corresponding Author
*Email: imamuddeenkabir@gmail.com

ORCID
Imamuddeen Kabir : 0009-0008-8632-1986
Gbenga Abidemi Olarinoye : 0000-0002-7034-0452

REFERENCES

[1] Touati, Z.; Pereira, M.; Araújo, R.E.; Khedher, A. Integration of Switched Reluctance Generator in a Wind Energy Conversion System: An Overview of the State of the Art and Challenges. Energies 2022, 15, 4743. https://doi.org/10.3390/en15134743.

[2] K. M. Anjanee, Solar-powered switched reluctance motor-driven water pumping system with battery support. IET Power Electronics published by John Wiley & Sons Ltd. The Institution of Engineering and Technology. DOI: 10.1049/pel2.12084. 2020.

[3] Han S, Diao K, Sun X. Overview of multi-phase switched reluctance motor drives for electric vehicles. Advances in Mechanical Engineering. 2021;13(9). doi:10.1177/16878140211045195.

[4] I. Al-Bahadly, An Integrated Wind and Hydro Power System Using Switched Reluctance Generator. Journal of Power and Energy Engineering, Vol.6 No.2, 2018.

[5] Kamali, Z. H., Salameh, Z., & Ashfaq, A. (2017). Modeling of wind energy conversion system using PSCAD/EMTDC. *International Journal of Renewable Energy Research*, 7(1), 178-187.

[6] Miller, T. J. E. (2001). Electronic control of switched reluctance machines: Elsevier.

[7] Hu, K.-W., Wang, J.-C., Lin, T.-S., & Liaw, C.-M. (2014). A switched-reluctance generator with interleaved interface DC-DC converter. IEEE Transactions on Energy Conversion, 30(1), 273-284.

[8] K. Nagesh, D. Leine, & P. Sujatha, Modelling and analysis of 8/6 switched reluctance motor with PI controller. Journal of Mechanics of Continua and Mathematical Sciences, 5, 357-370. 2020.

[9] Peng, W., Pelletier, J., Mollet, Y., & Gyselinck, J. (2018). Torque Sharing Function and Firing Angle Control of Switched Reluctance Machines-Hysteresis Current Control Versus PWM. Paper presented at the 2018 XIII International Conference on Electrical Machines (ICEM).

[10] Touati, Z., Mahmoud, I., & Khedher, A. (2020). Hysteresis Current Control of Switched Reluctance Generator. Paper presented at the 2020 11th International Renewable Energy Congress (IREC).

[11] Mapa, S., Maheswari, R., & Bhuvaneswari, G. (2018). Maximum power point tracking using a novel current control strategy in an SRG-based variable speed wind energy conversion system. Paper presented at the 2018 8th IEEE India International Conference on Power Electronics (IICPE).

[12] dos Santos Barros, T. A., dos Santos Neto, P. J., Nascimento Filho, P. S., Moreira, A. B., & Ruppert Filho, E. (2017). An approach for switched reluctance generator in a wind generation system with a wide range of operation speeds. IEEE Transactions on Power Electronics, 32(11), 8277-8292.

[13] Osman, M. A., Abdelsalam, A. K., & Dessouky, Y. G. (2021). Enhanced Wind Energy Conversion System Adopting Modified Switched Reluctance Generator Converter. Paper presented at the 2021 IEEE Fourth International Conference on DC Microgrids (ICDCM).

[14] Krishnan, R. (2017). Switched reluctance motor drives: modeling, simulation, analysis, design, and applications: CRC press.

[15] Soufi, Y., Kahla, S., Sedraoui, M., & Bechouat, M. (2016). Optimal control-based RST controller for maximum power point tracking of wind energy conversion system. Paper presented at the 2016 IEEE International Conference on Renewable Energy Research and Applications (ICRERA).

[16] Omaç, Z., & Cevahir, C. (2021). Control of switched reluctance generator in wind power system application for variable speeds. Ain Shams Engineering Journal. doi: https://doi.org/10.1016/j.asej.2021.01.009.
[17] Kurian, S., & Nisha, G. (2015). Torque ripple minimization of SRM using torque sharing function and hysteresis current controller. Paper presented at the 2015 International Conference on Control Communication & Computing India (ICCC).
[18] Hancco Catata, E. O., de Paula, M. V., dos Santos Neto, P. J., Ruppert Filho, E., Luque Carcasi, D. B., & dos Santos Barros, T. A. (2023). Direct average torque control of switched reluctance generator. IET Power Electronics.
[19] Rashid, M. H. (2007). Devices, circuits, and applications. In: Burlington: Academic Press.
[20] Patel, M. R., & Beik, O. (2021). Wind and solar power systems: design, analysis, and operation: CRC press.
[21] Ackermann, T., & Söder, L. (2002). An overview of wind energy-status 2002. Renewable and sustainable energy reviews, 6(1-2), 67-127.
[22] Ogunjuyigbe, A., Ayodele, T., Adetokun, B., & Jimoh, A. (2016). Dynamic performance of wind-driven self-excited reluctance generator under varying wind speed and load. Paper presented at the 2016 IEEE International Conference on Renewable Energy Research and Applications (ICRERA).
[23] Kahla, S., Soufi, Y., Sedraoui, M., & Bechouat, M. (2017). Maximum power point tracking of wind energy conversion system using multi-objective grey wolf optimization of fuzzy-sliding mode controller. *International Journal of Renewable Energy Research*, 7 (2), 926-936.
[24] Fernandes, N., Bindu, R., & George, S. (2016). Control of switched reluctance generator in the wind energy system. Paper presented at the 2016 Online International Conference on Green Engineering and Technologies (IC-GET).
[25] Bilgin, B., Jiang, J. W., & Emadi, A. (2019). Switched reluctance motor drives: fundamentals to applications: CRC press